Volume 13, Number 1, 2020. pp. 29-46

Jordan Journal of Physics

ARTICLE

Physical Properties of RhCrZ (Z= Si, Ge, P, As) Half-Heusler Compounds: A First-Principles Study

B. Amrani[a], **A. Chahed**[a], **M. Rahmoune**[a], **K. Benkaddour**[a] and **A. Sayede**[b]

[a] *Condensed Matter and Sustainable Development Laboratory (LMCDD), University of Sidi Bel-Abbes, Sidi Bel-Abbes 22000, Algeria.*

[b] *UCCS, CNRS-UMR 8181, Université d'Artois, Faculté des Sciences Jean Perrin, Rue Jean Souvraz, SP 18, 62307 Lens Cedex, France.*

Doi : 10.47011/13.1.3

Received on: 5/6/2019; *Accepted on: 7/11/2019*

Abstract: We use the first-principles-based density functional theory with full potential linearized augmented plane wave method in order to investigate the structural, elastic, electronic, magnetic and thermoelectric properties of RhCrZ (Z= Si, Ge, P, As) Half-Heusler compounds. The preferred configurations of the RhCrZ alloys are all type α. The structural parameters are in good agreement with the available theoretical results. The Young's and shear modulus, Poisson's ratio, sound velocities, Debye temperature and melting temperature have been calculated. Furthermore, the elastic constants C_{ij} and the related elastic moduli confirm their stability in the cubic phase and demonstrate their ductile nature. The compounds RhCrSi, RhCrGe, RhCrP and RhCrAs are found to be half-metallic ferrimagnets (HMFs) with a half-metallic gap E_{HM} of 0.37, 0.35, 0.25 and 0.02 eV, respectively. The half-metallicity of RhCrZ (Z= Si, Ge, P, As) compounds can be kept in a quite large hydrostatic strain and tetragonal distortion. The Curie temperatures of RhCrSi, RhCrGe, RhCrP and RhCrAs compounds are estimated to be 952, 1261, 82 and 297 K, respectively, in the mean field approximation (MFA). Thermoelectric properties of the RhCrZ (Z= Si, Ge, P, As) materials are additionally computed over an extensive variety of temperatures and it is discovered that RhCrAs demonstrates higher figure of merit than RhCrSi, RhCrGe and RhCrP. The properties of half-metallicity and higher Seebeck coefficient make this material a promising candidate for thermoelectric and spintronic device applications.

Keywords: Heusler alloys, Electronic structures, Magnetic properties, Mechanical properties.

Introduction

The scientific community is engaged in finding a material candidate that has a conversion efficiency as high as possible [1]. The Heusler alloys have been immensely studied with respect to thermoelectric technology due to their unique properties, like half-metallic ferromagnetism, topological insulation and Weyl semimetalicity [2]. They also possess a special spin band behavior, where one of the spin densities shows typically a metallic behavior while the other is semiconducting. Heusler alloys with chemical formulae of XYZ, X_2YZ and XX'YZ (where X, X', Y = transition metals, Z = *s*, *p* element) have been found to be potential candidates for spintronic applications [3].

The concept of half-metallic ferromagnets was first introduced by de Groot et al. [4], on the basis of band structure calculations in NiMnSb and PtMnSb semi-Heusler phases. Half-metallic materials have been found theoretically in many

Corresponding Author: Chahed Abbes **Email**: cha.abbes68@gmail.com

materials; for example, ferromagnetic metallic oxides [5], dilute magnetic semiconductors [6], zincblende compounds [7], full-Heusler compounds [8], half-Heusler compounds [9] and quaternary Heusler alloys [10].

Although numerous half-Heusler compounds have been predicted to be half-metallic by first-principles calculations [11-13], a comprehensive study of the structural, electronic and magnetic properties of the half-Heusler family is useful, because it is not clear which of the many half-metallic half-Heuslers that can be imagined are stable. Thus, a systematic study of the structural stability of the half-Heusler family should provide guidance for future experiments. Among these, the RhCrZ (Z= Si, Ge, P, As) compounds have not received much attention theoretically and experimental information on these compounds is also scarce.

Until now, no half-metallic gap E_{HM}, which is the minimum energy for the electron to change the spin, has been found in either theory or experiment investigations of these compounds. The characteristics of energy bands and origin of half-metallic gap were also not studied. In addition, the effect of volumetric and tetragonal strain on the half-metallicity character was not investigated. It is also interesting to estimate the Curie temperatures of the RhCrZ (Z= Si, Ge, P, As) half-Heusler compounds to see their potential application in spintronics. On the other hand, half-Heusler (HH) alloys are potential candidates for use in high-temperature thermoelectric materials [14-16]. HH compounds are also used for power generation, because they are cheaper, abundant in nature and environmentally friendly; i.e., free from toxic elements [17]. HH compounds have attracted attention, because they have high-power factors due to the combination of large Seebeck coefficients and moderately low electrical resistivity.

For all these reasons, we perform these calculations by using the full-potential augmented plane wave (FP-LAPW) in order to provide reference data for experimentalists and to complete existing theoretical works on these compounds. Our paper is organized as follows: theoretical background, results and discussion and a summary of the results.

Computational Method

The calculations were performed within the density functional theory (DFT) [18]. We use the full potential linear-augmented-plane waves plus local orbital (FP-LAPW) method [19], as implemented in the Wien2k package [20]. The exchange-correlation potential was treated under the generalized gradient approximation (GGA) [21]. The core and valence states were treated with the relativistic and scalar relativistic approach, respectively. The partial waves used inside the atomic spheres are expanded up to l_{max} = 10 with a matrix size $R_{mt}K_{max}$ equal to 8, where R_{mt} represents the smallest atomic sphere radii and K_{max} is the plane waves' cut-off. A 20x20x20 *k*-point mesh was used as base for which the first Brillouin zone was found to be sufficient in most cases. Within the (FP-LAPW) method, we impose a convergence criterion of 10^{-5} in the total energy and charge density to improve accuracy in the spin-polarized calculations.

Results and Discussion

Structural Properties

In general, half-Heusler alloys, XYZ, have $C1_b$ structure [22], which is similar to the structure of a full-Heusler alloy (X_2YZ), the $L2_1$ structure, except missing one X. The elements of X and Y are alkali metals, transition metals or rare-earth metals and Z is a main group element. The Z atoms constitute the most electronegative part of the half-Heusler XYZ compounds, followed by the X atoms, leaving the Y atom as the electron donating constituent. The X_2YZ full-Heusler $L2_1$ type structure consists of four fcc sublattices. The unit cell contains four atomic positions, X at (0,0,0) and (1/2,1/2,1/2),Y at (1/4,1/4,1/4) and Z at (3/4,3/4,3/4). Due to missing one X atom, there are three atomic configurations for XYZ half-Heusler alloys, which are called α, β and γ types; type α: X (0.25, 0.25, 0.25), Y (0, 0, 0) and Z (0.5, 0.5, 0.5); type β: X (0.25, 0.25, 0.25), Y (0.5, 0.5, 0.5) and Z (0, 0, 0); type γ: X (0.5, 0.5, 0.5), Y (0.25, 0.25, 0.25) and Z (0, 0, 0). In all three atomic configurations, the (0.75, 0.75, 0.75) site is empty.

In the first step, in order to obtain the correct atomic arrangement and the magnetic ground state corresponding to the true ground state of the half-Heusler RhCrZ (Z= Si, Ge, P, As) compounds, we performed the energy minimization as a function of lattice constant with respect to the three different possible site occupations for every non-magnetic (NM), ferromagnetic (FM) and antiferromagnetic (AFM) configurations and the obtained curves are shown in Fig. 1 and Fig. 2. The calculated total energies within GGA as a function of volume are fitted to Murnaghan's equation of state to obtain the ground-state properties [23].

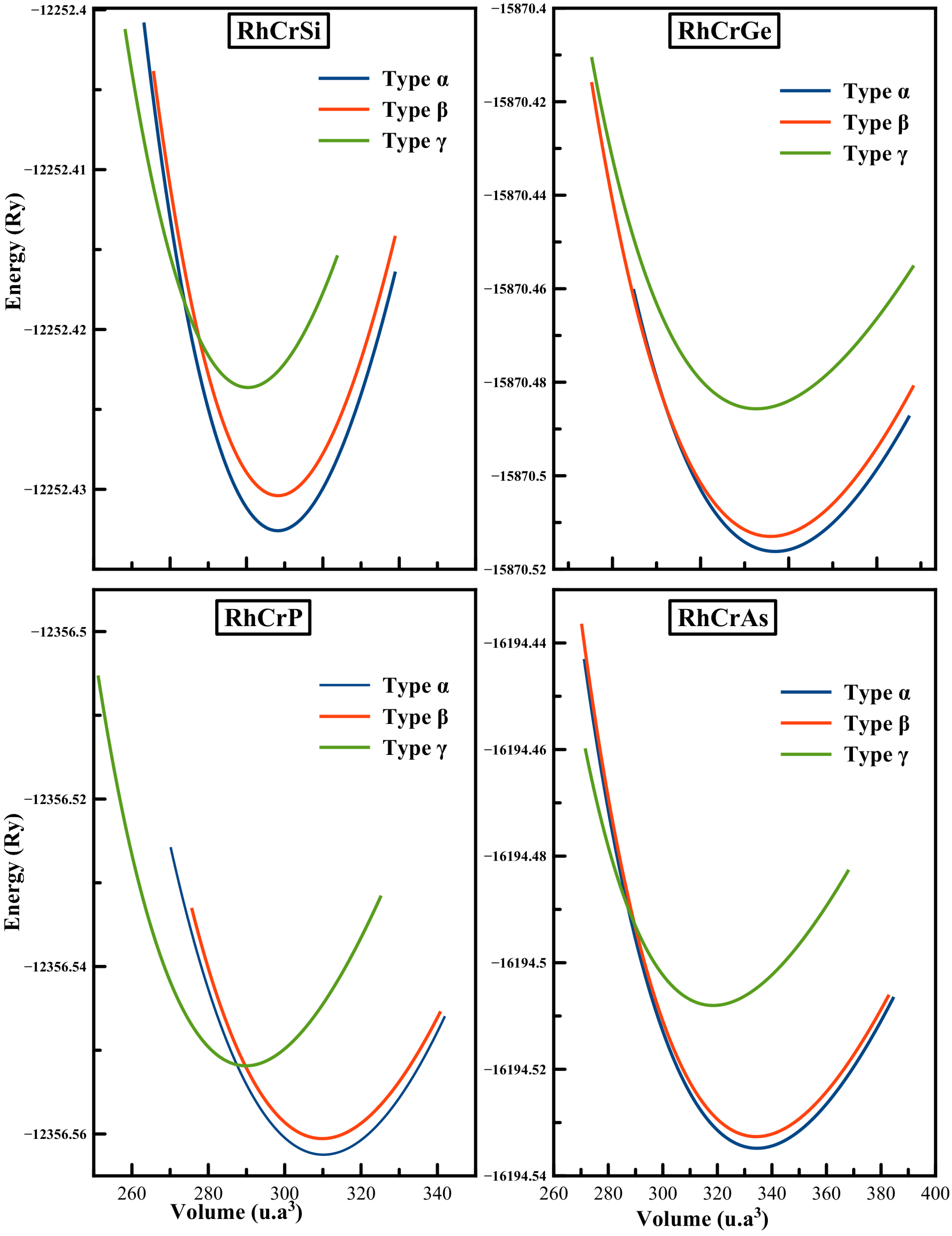

FIG. 1. Total energy as a function of volume per formula unit (f.u.) in the three atomic arrangements: type α, type β and type γ for the RhCrZ (Z= Si, Ge, P, As) compounds. The curves correspond to the FM state.

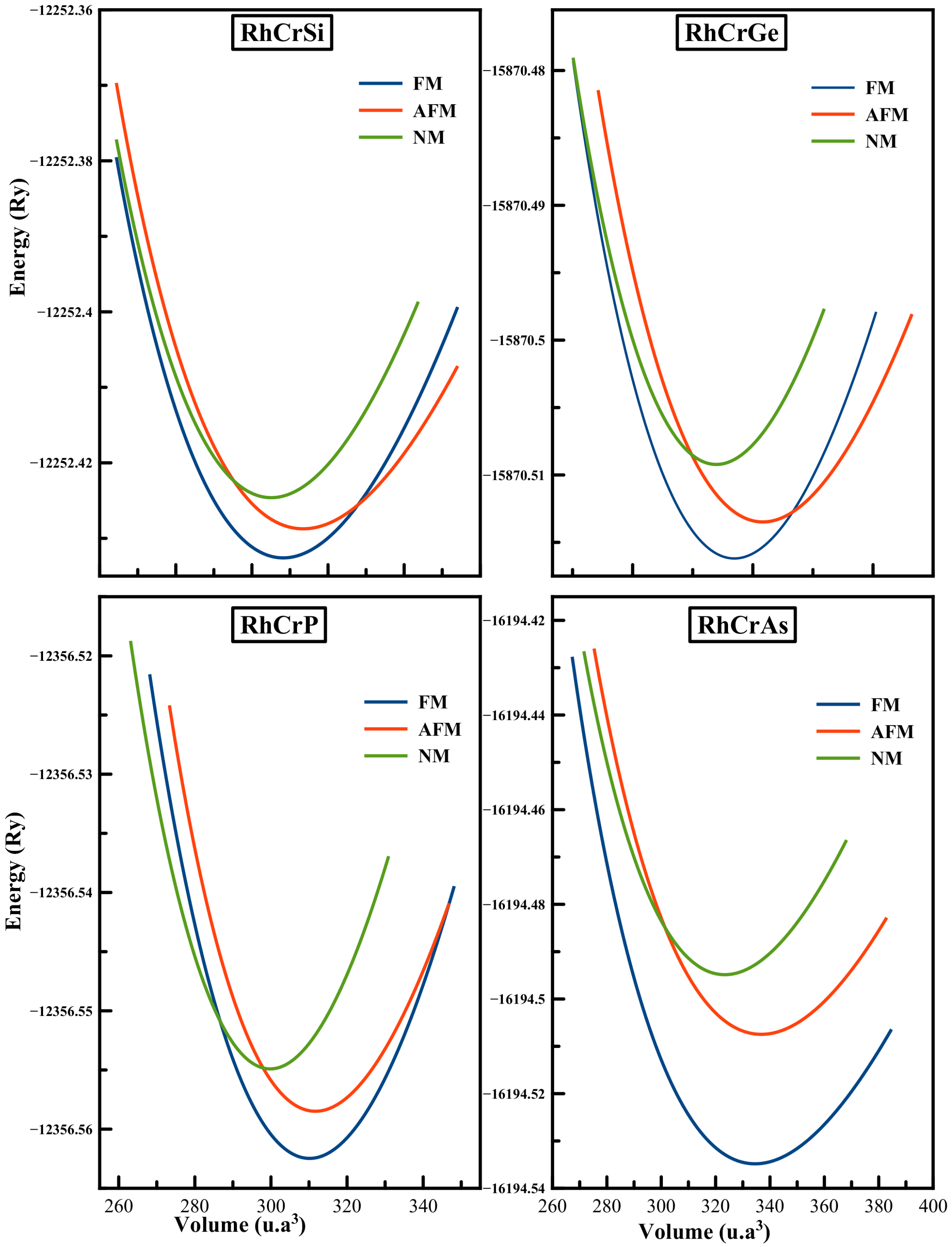

FIG. 2. Total energy as a function of volume per formula unit (f.u.) in the three magnetic states: FM, AFM and NM for the RhCrZ (Z= Si, Ge, P, As) compounds. The curves correspond to the type α structure.

As seen in Figs. (1,2), the optimization of the cubic lattice parameters for all three possible configurations in their respective three different magnetic configurations revealed the lowest energy for *type* α structure with a ferromagnetic ground state for all compounds (type α + *FM*). The obtained equilibrium lattice constants, bulk modulus and the corresponding total energies are presented in Table 1.

TABLE 1. Calculated total energies E_{tot} (in Ry) per formula unit, equilibrium lattice constant a_0 (in Å), the bulk modulus B (in GPa) and formation energy E_f (in Ry) for RhCrZ (Z= Si, Ge, P, As) half-Heusler compounds in their different structure types and magnetic configurations.

Compound	Structure	E_{tot} (Ry)			a_0 (Å)	B (GPa)	E_f (Ry)
		NM	FM	AFM	FM	FM	FM
RhCrSi	Type α	-12252.424612	-12252.432589	-12252.428423	5.6742	185.0286	-1.71
	Type β	-12252.424521	-12252.432396	-12252.430944	5.6745 5.65 [a] 5.65 [b]	184.4734 408.1[b]	-1.697 -2.486[a]
	Type γ	-12252.384913	-12252.423623	-12252.407615	5.6279	154.8741	-1.669
RhCrGe	Type α	-15870.509219	-15870.516193	-15870.513548	5.7776	168.7817	-1.585
	Type β	-15870.504840	-15870.513131	-15870.492267	5.7795 5.75[a] 5.76[b]	144.9142 173.04[b]	-1.573 -0.761[a]
	Type γ	-15870.479146	-15870.485676	-15870.481536	5.8613	140.2142	-1.511
RhCrP	Type α	-12356.554924	-12356.562472	-12356.558487	5.686	171.0891	-1.707
	Type β	-12356.530538	-12356.560651	-12356.553949	5.6842 5.65[a] 5.67[c]	171.5793 224.6[c]	-1.696 -3.981[a]
	Type γ	-12356.473652	-12356.551856	-12356.548623	5.7363	135.4124	-1.672
RhCrAs	Type α	-16194.494862	-16194.534822	-16194.507464	5.8312	145.2174	-1.608
	Type β	-16194.494837	-16194.532635	-16194.507476	5.8294 5.81[a] 5.80[c]	144.7208 206.00[c]	-1.550 -1.644[a]
	Type γ	-16194.502575	-16194.508025	-16194.506468	5.7363	135.4124	-1.558

[a] [24], [b] [25], [c] [26]

Until now, there are no other experimental or theoretical results in the structure type α and only very few theoretical results have been reported for these compounds in the structure type β [24-26], which is not the most stable state, as shown in Figs. (1,2). However, this structure type β is closer to the structure type α than the structure type γ, as shown in Fig. 1 and Table 1. Our optimized lattice constants for our compounds show very good agreement with the recent available theoretical results [24-26] listed in Table 1. We believe that our calculated results are reliable and we propose a future experimental work to verify our calculated results. The highest calculated bulk moduli for RhCrZ (Z= Si, Ge, P, As) in type α + FM configuration confirm the stability of this structure.

The formation energy E_f determines whether a compound can be experimentally synthesized or not. E_f is the change in energy when a material is formed from its constituent elements in their bulk states and can be calculated for RhCrZ (Z= Si, Ge, P, As) compounds as:

$$E_f^{RhCrZ} = E_{tot}^{RhCrZ} - \left(E_{Rh}^{Bulk} + E_{Cr}^{Bulk} + E_Z^{Bulk} \right); \quad \mathrm{Z = Si\ Ge, P\ As} \qquad (1)$$

where E_{tot}^{RhCrZ} represents the first-principles calculated equilibrium total energy of the studied compounds per formula unit, E_{Rh}^{bulk}, E_{Cr}^{bulk} and E_Z^{bulk} are the equilibrium total energies per atom of the pure constituent elements Rh, Cr, Si, Ge, P and As in their individual stable bulk structures. In Table 1, we give the values of formation energy for all types of structures and all magnetic configurations. The negative sign of formation energy values for the four alloys reported in this study implies that they can be experimentally fabricated. Also, according to Table 1, the calculated E_f values confirm the structural stability of type α +FM structure for all RhCrZ (Z= Si, Ge, P, As) compounds (high negative formation energy). Among them, RhCrSi is most easily synthesized because of its lowest formation energy. Based on this, all the further calculations on elastic, thermal, electronic, magnetic and thermoelectric properties of RhCrZ (Z= Si, Ge, P, As) were performed on this structure only; i.e in the type α +FM structure.

Elastic Properties

To confirm the stability of the studied compounds, the elastic properties have been studied. Since RhCrZ (Z= Si, Ge, P, As) compounds have cubic symmetry, we have calculated only three independent elastic parameters; C_{11}, C_{12} and C_{44}. The obtained elastic constant values for RhCrZ (Z= Si, Ge, P, As) compounds are given in Table 2. The bulk modulus values calculated from the theoretical values of the elastic constants $B = (1/3)\,(C_{11} + 2C_{12})$ is also listed in Table 2. The traditional mechanical stability conditions of the elastic constants in cubic crystal [27] are:

$$(C_{11} + 2C_{12}) > 0; \quad \frac{1}{2}(C_{11} - C_{12}) > 0;$$

$$C_{11} > 0;\ C_{44} > 0;\ C_{12} < B < C_{11} > 0 \qquad (2)$$

Thus, these compounds are elastically stable as satisfying these restrictions indicating that the *α-type +FM* structure is a mechanically stable phase. It may be noted that the value of *B* (bulk modulus) calculated from the elastic constants has nearly the same value as the one obtained from energy minimization. This gives a good estimate of the precision and accuracy of the elastic constants' calculations performed in this article of our compounds.

TABLE 2. Calculated elastic constants C_{ij} (in GPa), Calculated Voigt shear modulus G_V (in GPa), Reuss shear modulus G_R (in GPa), shear modulus *G* (in GPa), bulk modulus *B* (in GPa), Young's modulus *Y* (in GPa), Poisson's ratio *ν*, anisotropy factor *A* and *B/G* ratio for RhCrZ (Z= Si, Ge, P, As) compounds.

Compound	C_{11}	C_{12}	C_{44}	G_V	G_R	*G*	*B*	*Y*	*ν*	*A*	*B/G*
RhCrSi	223.7255	168.951	123.7067	85.178	51.399	68.288	187.208	182.654	0.337	4,517	2.7414
	247.32 ^{b}	165.46 ^{b}	137.66 ^{b}			87.48		227.84 ^{b}	0.30 ^{b}	3.35 ^{b}	2.20 ^{b}
RhCrGe	222.348	142.4235	123.2154	89.913	67.208	78.56	169.064	204.071	0.298	3.084	2.152
	277.50^b	125.14 ^{b}	117.48 ^{b}			98.7 ^{b}		249.4 ^{b}	0.26 ^{b}	1.53 ^{b}	1.78 ^{b}
RhCrP	192.8669	166.2601	96.0693	62.962	27.538	45.25	175.128	124.985	0.381	7.221	3.87
	261.08 ^{c}	206.53 ^{c}	108.85 ^{c}	108.50 ^{c}	49.50 ^{c}			35.50 ^{c}	0.38 ^{c}	3.99 ^{c}	2.38 ^{c}
RhCrAs	161.0483	121.2655	104.2189	70.487	38.66	54.573	134.526	144.217	0.321	5.24	2.465
	249.82 ^{c}	184.60 ^{c}	115.80 ^{c}	82.00 ^{c}	57.00 ^{c}			187.00 ^{c}	0.34 ^{c}	3.50 ^{c}	2.90 ^{c}

^{a} [24] , ^{b} [25] , ^{c} [26].

From Table 2, it was observed that the C_{11} constant for the four half-Heusler compounds is larger than the C_{44} constant, which implies that the investigated compounds present a weaker resistance to pure shear deformation compared to the resistance to unidirectional compression. The elastic anisotropy parameter *A* plays an important role in engineering sciences to detect the micro-cracks in materials. The deviation from 1 shows the degree of elastic anisotropy possessed by a crystal. The obtained elastic constants are used to compute the anisotropy constant *A* [27], which is given by $A = 2\,C_{44}/(C_{11}- C_{12})$. According to the values of *A* listed in Table 2, all our RhCrZ (Z= Si, Ge, P, As) compounds show anisotropic behaviour and possess a low probability to develop micro-cracks or structural defects during their growing process. Also, we can clearly observe that the anisotropy decreases on insertion of the anion with large atomic size for each *IV* and *V* column, respectively. RhCrP is characterized by a strong anisotropy compared to the other three compounds. The main isotropic mechanical parameters; namely, bulk modulus *B*, shear modulus *G*, Young's modulus *Y* and Poisson's ratio *ν*, which are the important elastic moduli for applications, are calculated from the elastic constants C_{ij} of the single crystal using the Voigt–Reuss–Hill approximation [28] by the following relations:

$$G_V = \frac{1}{5}\,(C_{11} - C_{12} + 3C_{44}) \qquad (3)$$

$$G_R = \frac{5C_{44}(C_{11}-C_{12})}{4C_{44}+(C_{11}-C_{12})} \qquad (4)$$

$$B_V = B_R = \frac{1}{3}(C_{11} + 2C_{12}) \qquad (5)$$

$$G = \frac{1}{2}(G_V + G_R) \qquad (6)$$

The Young's modulus *Y* and Poisson's ratio *ν* were calculated, which are related to the bulk modulus *B* and the shear modulus *G* by the following equations:

$$Y = \frac{9BG}{(3B+G)} \qquad (7)$$

$$\nu = \frac{(3B-2G)}{2\,(3B+G)} \qquad (8)$$

Our results on Young's modulus (*Y*), shear modulus (*G*) and Poisson's ratio (*ν*) of the four compounds using GGA are listed in Table 2. Shear modulus (*G*) and Young modulus (*Y*) can be considered as stiffness indicators. Our calculations of *G* and *Y* show clearly that RhCrGe is stiffer than RhCrSi → RhCrAs → RhCrP.

Having acquired the necessary data, three parameters are used to estimate the ductile or brittle nature of these compounds. The Cauchy pressure (C_{12} - C_{44}), Pugh's index of ductility (*B/G*) and Poisson's ratio (ν). Present values of Cauchy pressure (C_{12} - C_{44}) for all our compounds RhCrZ (Z= Si, Ge, P, As) are positive; therefore, these compounds are ductile in nature. According to Pugh criterion [29], the critical value (*B/G*) which separates the ductile and brittle was found to be 1.75. As mentioned in Table 2, this ratio is greater than 1.75 for all our compounds RhCrZ (Z= Si, Ge, P, As), which are classified as ductile materials. For brittle materials, the Poisson's ratio is less than 0.26; otherwise the material behaves in a ductile manner. The results displayed in Table 2 show that all our compounds RhCrZ (Z= Si, Ge, P, As) are also classified as ductile alloys. These different results are in overall agreement with the other theoretical results found for type β [25, 26] and reported in Table 2.

Thermal Properties

Study of thermal properties provides information about phase stability, melting point, strength and bonding nature, among other properties. We estimated that the Debye temperature θ_D performs a central role in determining thermal characteristics of materials as well as in the development and manufacturing of electronic devices. Also, Debye temperature is used to distinguish between high- and low-temperature regions in solids. As a rule of thumb, a higher θ_D implies a higher melting temperature and thermal conductivity. The Debye temperature (θ_D) can be estimated from the average sound velocity, v_m, by the following classical relation [30]:

$$\theta_D = \frac{h}{k}\left[\frac{3n}{4\pi}\left(\frac{\rho N_A}{M}\right)\right]^{1/3} v_m \tag{9}$$

where h and k are the Plank's and Boltzmann's constants, respectively, n is the number of atoms per formula unit, N_A is the Avogadro's number, ρ is the density of the compound, M is the molecular mass per formula unit and v_m is the average wave velocity [30] which is given by:

$$v_m = \left[\frac{1}{3}\left(\frac{2}{v_t^3} + \frac{1}{v_l^3}\right)\right]^{-1/3} \tag{10}$$

where v_l and v_t, are the longitudinal and transverse elastic wave velocities, respectively, which are obtained from Navier's equations [30]:

$$v_l = \left(\frac{3B+4G}{3\rho}\right)^{1/2} \tag{11}$$

$$v_t = \left(\frac{G}{\rho}\right)^{1/2} \tag{12}$$

The melting temperature (T_{melt}) is calculated from C_{11} using the following expression [30]:

$$T_{melt} = \left[553K + \left(\frac{5.91K}{GPa}\right)C_{11}\right] \tag{13}$$

The calculated Debye temperature, longitudinal, transverse and average elastic wave velocities and melting temperature at zero pressure for the present compounds are given in Table 3. In light of these results, the Debye temperature and the melting temperature are directly related to elastic constants and decrease from RhCrSi to RhCrGe and from RhCrP to RhCrAs, respectively. To the best of our knowledge, there is no other theoretical and experimental data existent for comparison. Anyway, further experimental works are desirable.

TABLE 3. The calculated sound velocity longitudinal v_l (in m.s^{-1}), sound velocity transverse v_t (in m.s^{-1}), average sound velocity v_m (in m.s^{-1}), Debye temperature θ_D (in K) and melting temperature T_{melt} (in K) for RhCrZ (Z= Si, Ge, P, As) compounds.

Compound	v_l	v_t	v_m	θ_D	T_{melt}
RhCrSi	6467.07	3203.73	3595.92	431.965	1875.2177
RhCrGe	5910.97	3166.17	3536.01	417.163	1867.0766
RhCrP	5921.09	2595.68	2930.73	351.324	1692.8433
RhCrAs	5189.29	2662.61	2982.24	348.578	1504.7954

Electronic Properties

The electronic band structure calculations are done to predict the electronic nature of RhCrZ (Z= Si, Ge, P, As) compounds. The majority and minority spins (spin-up and spin-down) band structure along the high symmetry direction of the first Brillouin zone are depicted in Fig. 3 (a-d) for RhCrSi, RhCrGe, RhCrP and RhCrAs, respectively. As can be seen in Fig. 3, all RhCrZ (Z= Si, Ge, P, As) compounds have shown half-metallicity, because the spin-up (majority) band structure has metallic intersections at the Fermi level, indicating clearly strong metallic nature, whereas the spin-down (minority) band structure exhibits a semiconductor behavior. Fig. 3 shows that in minority spin channel, all four compounds have an indirect band gap E_g (Γ- X). The half-metallic gap E_{HM} is defined as the minimum energy required to flip a minority-spin electron from the valance band maximum to the majority-spin Fermi level, as listed in Table 4. The calculated band gap values for the investigated compounds are listed in Table 4, along with the other previous theoretical calculations. The half-metallic gap $\mathrm{E_{HM}}$ is strongly influenced by group IV elements (Si,Ge) and group V ones (P,As) and decrease from RhCrSi to RhCrGe and from RhCrP to RhCrAs, respectively. It is clearly seen that the calculated indirect band gaps (Γ-X) are slightly larger than those obtained by M. Jianhua et al. [24] and are usually closes than those obtained by N. Mehmood et al. [25] and R. Ahmad et al. [26]. Unfortunately, so far, no experimental measurements for band gap E_g and no experimental or theoretical data for the half-metallic gap E_{HM} for the investigated compounds have been carried out to compare with. Our total magnetic moment per formula unit values calculated are found to be integer values (see Table 4); $1.00\mu_B$ and $2.00\mu_B$ for RhCrZ (Z=Si,Ge) and RhCrZ (Z=P,As), respectively, and obey the Slater-Pauling behavior of HM ferromagnets [31], $M_{tot} = (Z_{tot} -18)$; here, M_{tot} and Z_{tot} are the total magnetic moment and the number of total valence electrons. Z_{tot} is 19 and 20 for RhCrZ (Z=Si,Ge) and RhCrZ (Z=P,As), respectively. In order to analyze the magnetic configurations of the half-metallic half-Heusler compounds, we also list in Table 4 the local magnetic moments at Rh, Cr and Z (Z=Si, Ge, P, As) sites. As seen in Table 4, for all four half-metal compounds, the main contribution to the total magnetic moment is due to the relatively large moment on the Cr sub-lattice with much smaller antiferromagnetically aligned moments on the Rh sub-lattice. The increase in atomic number of Z elements causes weak hybridization, yielding the enhancement of the local magnetic moment at the Cr site. The small moments on Rh are due to the difficulty in magnetically polarizing Rh atoms and the magnetic moment on the Z (Z= Si, Ge, P, As) atoms are quite small. A small amount of magnetic moment is found in the interstitial region too. To explain the magnetic properties in these compounds, we calculate the spin-polarized total densities of states (spin-TDOS) and partial density of states (spin–PDOS) of the RhCrZ (Z= Si, Ge, P, As) compounds at their optimized lattice constant presented in Fig. 4 and Fig. 5. As it can be seen, the general structure total TDOS is similar in shape for our compounds. At the first glance, it can easily be visualized that total DOS is mainly contributed by the 3*d* states of Cr and 4*d* states of Rh, while *p* state of Z (Z= Si, Ge, P, As) near the E_F makes no significant contribution to the total DOS. For example, in RhCrGe compound, the large exchange splitting of the Cr-3*d* states leads to a large magnetic moment of $1.251\mu_B$ at the Cr site. The exchange splitting of the Rh-4*d* states is relatively small and induces a magnetic moment of $-0.163\mu_B$. The DOS of Ge atom is almost symmetrical, yielding a very small magnetic moment of $-0.075\mu_B$.

The total DOS (spin-TDOS) of the RhCrZ (Z= Si, Ge, P, As) compound has a gap in the minority spin states at the Fermi level. The origin of the band gap may be attributed to the strong hybridization between the Cr-3*d* and Rh-4*d* electrons. In addition, since the total DOS of our compounds is generally similar in shape, we can conclude that the Z element is not responsible for the band gap. However, the substitutions of Z element result in a shift in the Fermi levels. On the other hand, the reason of the absence of a semiconducting gap in the majority spin is due to the dominance of the Cr-3*d* and Rh-4*d* electrons with little contribution of Z-*p* around the E_F for all the RhCrZ materials.

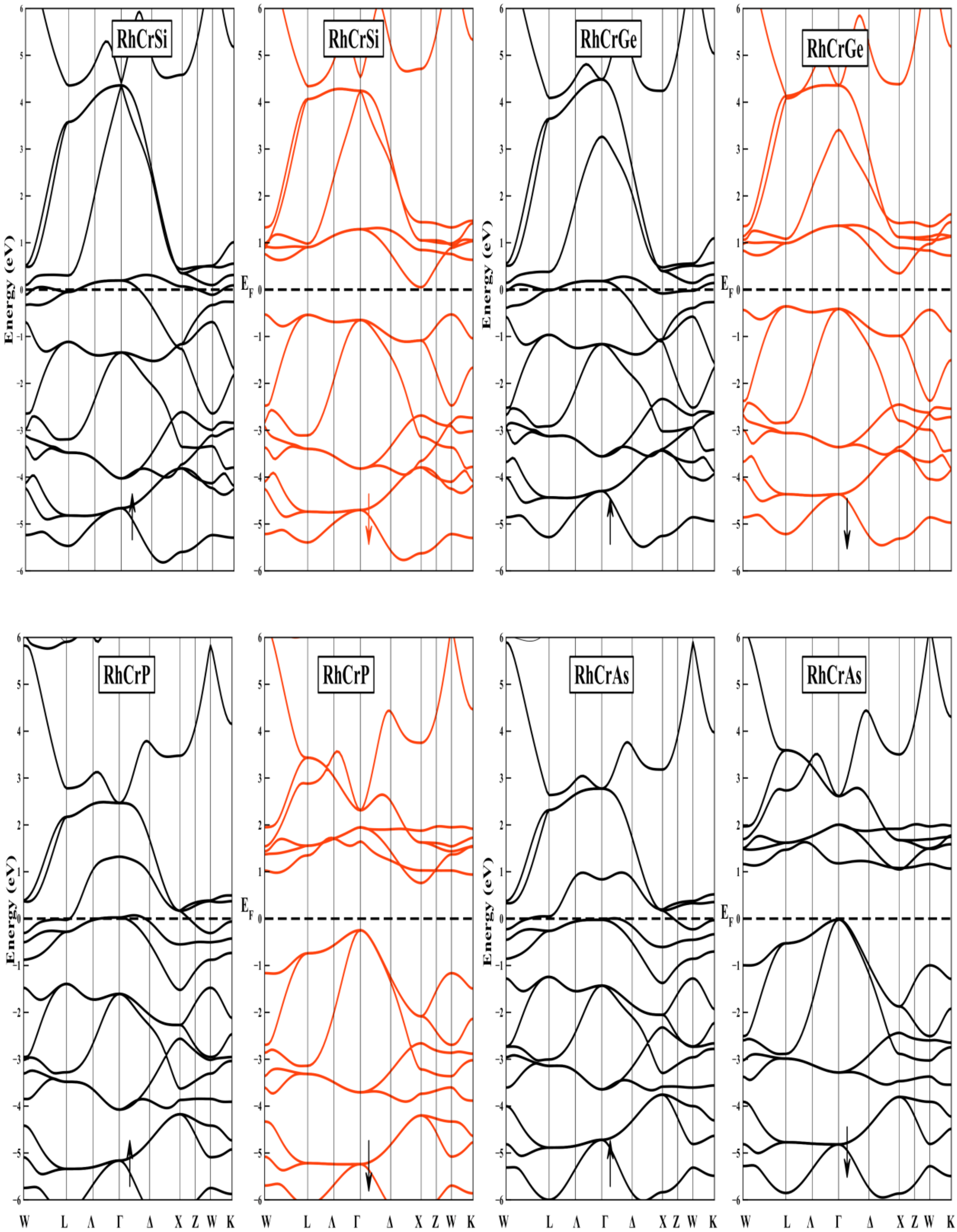

FIG. 3. Spin polarized band structure for the RhCrZ (Z= Si, Ge, P, As) compounds at their equilibrium lattice constants.

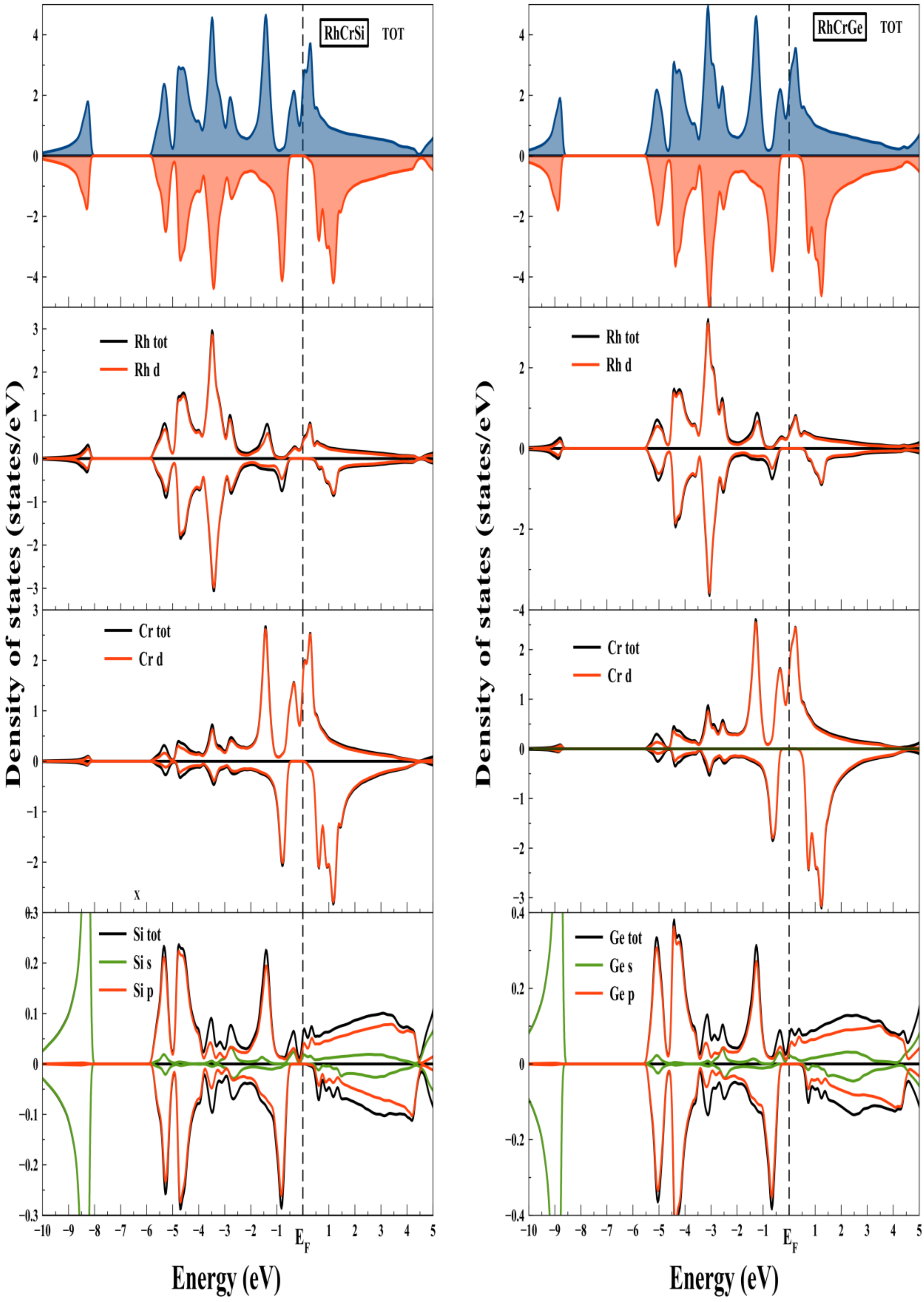

FIG. 4. Spin-polarized total and partial densities of states (DOS and P-DOS) of RhCrZ (Z= Si, Ge).

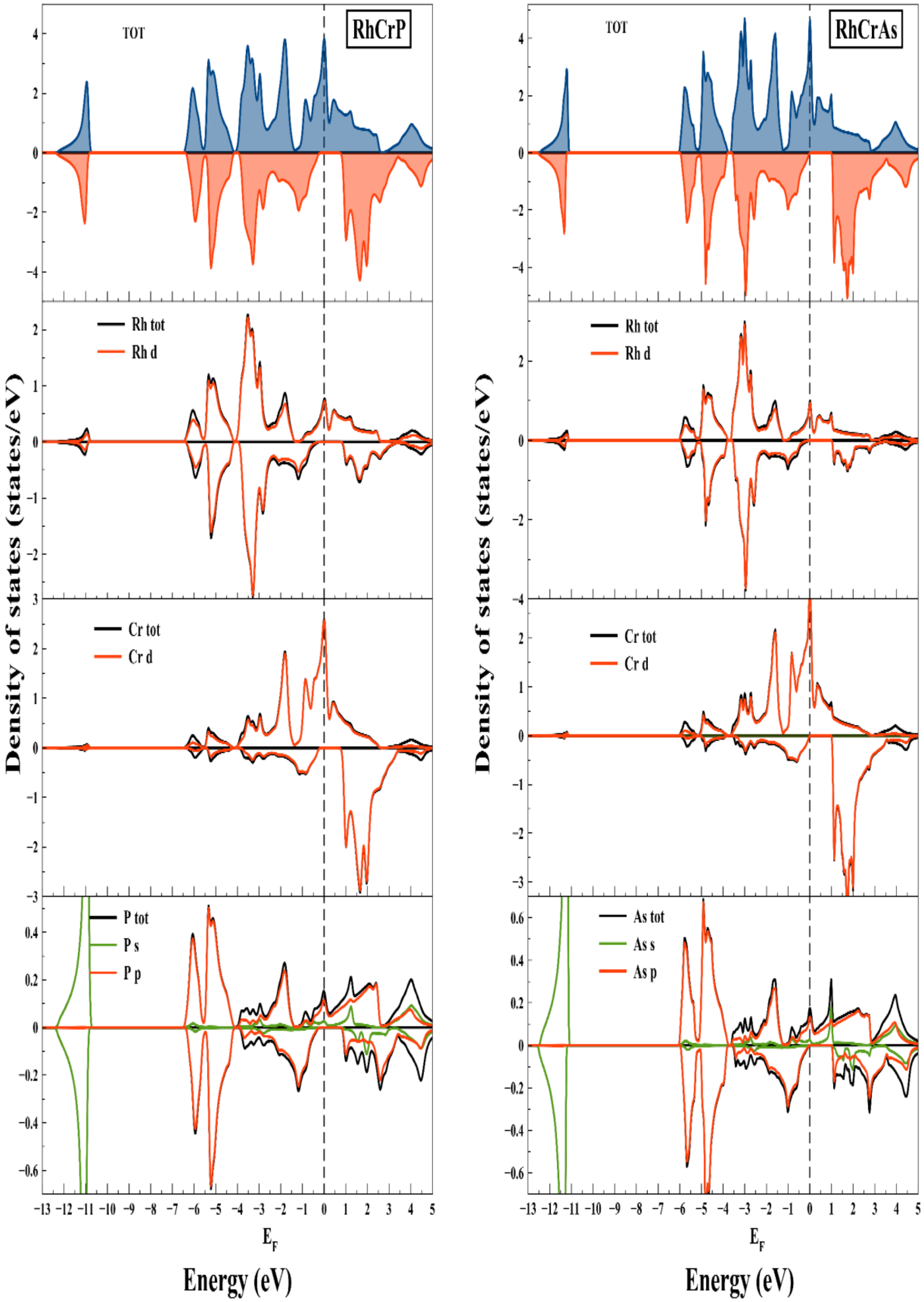

FIG. 5. Spin-polarized total and partial densities of states (DOS and P-DOS) of RhCrZ (Z= P, As).

TABLE 4. The semiconducting gap $E_g^{\Gamma\text{-}X}$ (in eV), the half-metallic gap E_{HM} (in eV), total magnetic moment μ_{tot} (in μ_B), magnetic moment per atom (Rh, Cr, Si, Ge, P, As), magnetic moment in the interstitial region μ_{int} and Curie temperature T_c (in K) in compounds RhCrZ (Z= Si, Ge, P, As).

Compound	E_g	E_{HM}	μ_{tot}	μ_{Rh}	μ_{Cr}	μ_Z	μ_{int}	T_c (°K)
RhCrSi	0.95	0.37	1	-0.113	1.182	-0.051	-0.018	951.163
	0.57[a]		1[a]	-0.148[a]	1.23[a]	-0.093[a]		
	0.26[b]		0.94[b]	-0.22[b]	1.28[b]	-0.05[b]	-0.06	
RhCrGe	0.71	0.35	1	-0.163	1.251	-0.075	-0.013	1261
	0.67[a]		1[a]	-0.191[a]	1.293[a]	-0.098[a]		
	0.82[b]		0.97[b]	-0.11[b]	1.17[b]	-0.05[b]	-0.03	
RhCrP	1.01	0.25	2	-0.204	2.214	-0.085	0.075	81.436
	0.91[a]		2[a]	-0.234[a]	2.297[a]	-0.121[a]		
	1.49[c]		2[c]	-0.13[c]	2.13[c]	-0.07[c]	0.08[c]	
RhCrAs	1.06	0.02	2	-0.249	2.299	-0.111	0.061	296.4
	0.95[a]		2[a]	-0.291[a]	2.384[a]	-0.135[a]		
	1.07[c]		2[c]	-0.15[c]	2.35[c]	-0.04[c]	0.06[c]	

[a] [24] , [b] [25] , [c] [26]

Because half-metallic materials are usually prepared as thin films for spintronic applications, where the lattice constant of the half-metallic material strongly depends on the substrate lattice parameter and correspondingly the half-metallicity may be destroyed. The effect of the change of lattice constant (uniform strain) on the electronic and magnetic properties was preformed to test the robustness of the half-metallic properties in RhCrZ (Z= Si, Ge, P, As) alloys. The half-metallicity represented by the variations of the valence band maximum (VBM) and the conduction band minimum (CBM) in the spin-down direction as a function of lattice constant is exhibited in Fig.6(a). From Fig. 6(a), we can see that the RhCrSi, RhCrGe, RhCrP and RhCrAs Heusler alloys will maintain their half-metallic nature with the lattice constants in the wide range of 5.483 – 6.06 Å, 5.56 – 6.07 Å, 5.37 – 5.85 Å and 5.32 – 5.85 Å corresponding to -3.37% – 6.8%, -3.77% – 5.06%, -5.56% – 5.69% and -8.77% – 0.37%, respectively. As it can be seen, the half-metallicity of RhCrGe and RhCrP is more robust against lattice constant change than that of RhCrSi and RhCrAs equilibrium lattice constant. On the other hand, in the RhCrAs (RhCrSi) compounds, although their half-metallic gap E_{HM} is small, the half-metallicity is found to be more robust with respect to the lattice compression (expansion) and is maintained up to the lattice constant contraction of 8.77% (expansion of +6.8%), compared with both other compounds RhCrGe and RhCrP.

Compared to the uniform strain, the tetragonal distortion (in-plane strain) is more practical in potential spintronic applications. In fact, in the growth of thin films, the tetragonal distortion with fixed volume is most likely to occur and is one of the most undesired troubles for the growing process. To study the effect of a tetragonal distortion with the c/a ratio, the variations of valence band maximum (VBM) and conduction band minimum (CBM) as a function of the c/a ratio for the RhCrZ (Z= Si, Ge, P, As) compounds are shown in Fig. 6(b). We keep the unit-cell volume the same as the equilibrium bulk volume ($a\times a\times a = a^3$). It can be seen that the half-metallic character appears to exhibit a low sensitivity to a tetragonal distortion of lattice structure mainly for both RhCrGe and RhCrP compounds. In detail, the RhCrSi, RhCrGe, RhCrP and RhCrAs compounds can maintain their half-metallicity when the c/a ratio changes within the range 0.893 - 1.156, 0.85 - 1.19, 0.83 - 1.26 and 0.99 - 1.03, respectively. The CBM, VBM and band gap of minority spin channel are approximately maximum at the equilibrium lattice constant and the absolute values of them decrease monotonically with both positive and negative tetragonal strain.

Since the equilibrium lattice constants of RhCrSi (5.6742 Å), RhCrP (5.686 Å), RhCrGe (5.7776 Å) and RhCrAs (5.8312 Å) compounds are close to those of zinc blende semiconductors, such as GaAs (5.65 Å) and CdS (5.818 Å) [32], it is suggested to grow new HM Heusler alloys in the form of thin films on suitable substrates to get new candidates for spintronic applications.

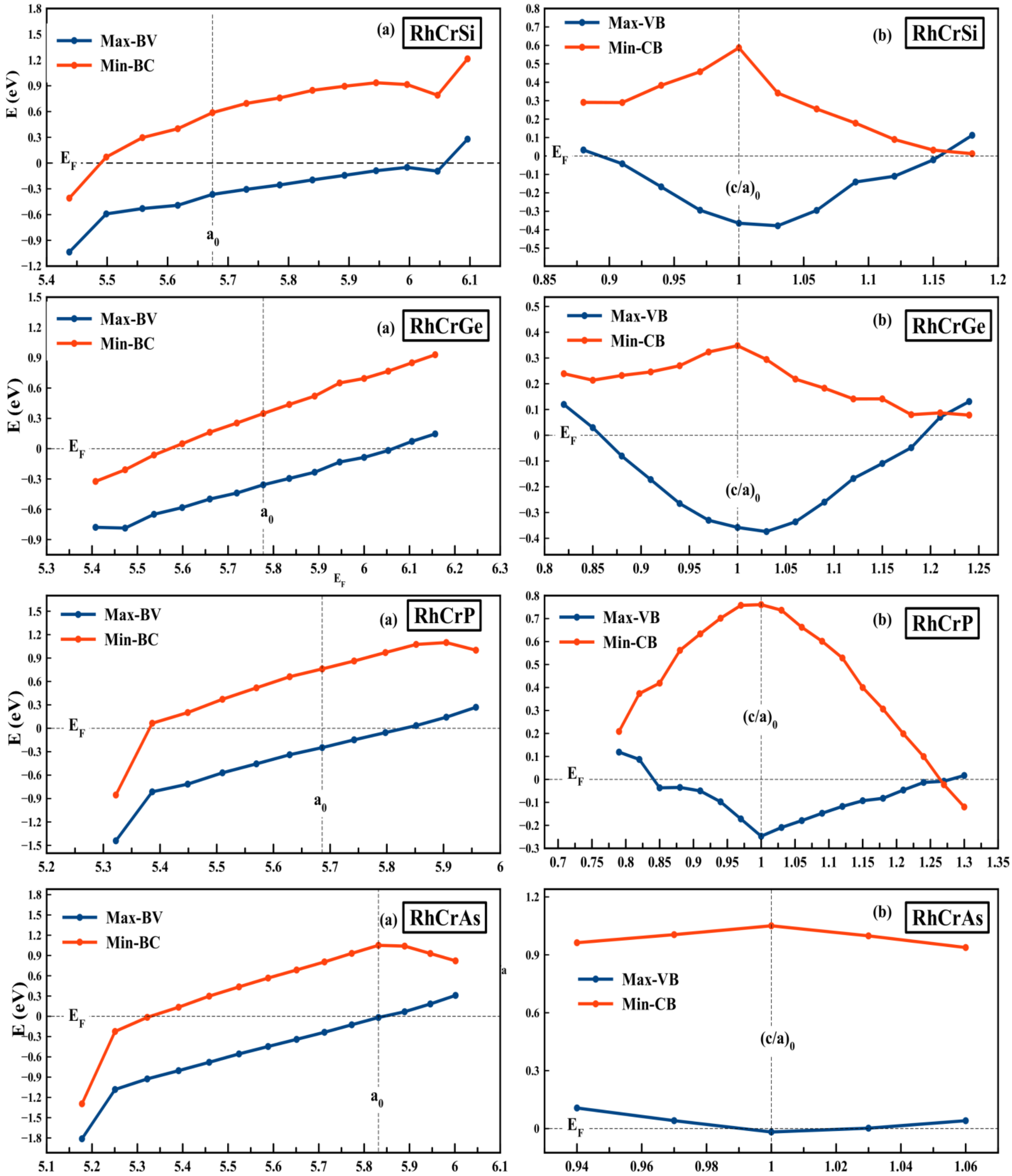

FIG. 6. Dependence of the *HM* state on the lattice constant (uniform strain) (a) at the c/a ratio (tetragonal distortion) (b) of RhCrZ (Z= Si, Ge, P, As) compounds. The blue lines correspond to the valence band maxima and the red lines correspond to the conduction band minima in the minority spin states (spin-down states).

The Curie temperature is another important aspect of application for spintronic materials. Using the mean field approximation (MFA) [33], the Curie temperature (T_C) can be calculated as:

$$T_c = \frac{2\Delta E}{3k_B} \qquad (14)$$

where ΔE is the total energy difference between the antiferromagnetic and ferromagnetic states ($\Delta E = E_{AFM} - E_{FM}$) *and* k_B is the Boltzmann constant. The results are given in Table 4. The Curie temperature has been calculated to be 81.436 K, 296.4 K, 951.163 K and 1261 K for RhCrP, RhCrAs, RhCrSi and RhCrGe, respectively. The Curie temperature *Tc* is strongly influenced by group IV elements (Si,Ge) and group V ones (P,As) and increases from RhCrSi to RhCrGe and from RhCrP to RhCrAs compounds, respectively. Among the four studied compounds, RhCrSi and RhCrGe seem to be the most suitable for applications, since they show the largest T_C. The Curie temperature of the half-metallic Mn_2VAl compound, estimated by using the mean field approximation, is 638 K and its value is in good agreement with the experimental value of the Curie temperature of 760 K [33].

Thermoelectric Properties

Thermoelectric (*TE*) materials transform the waste heat energy into usable electric energy, thereby offering a possible solution to the present-day energy crisis. This category of materials is currently being investigated at faster rates than other technologically important materials because of their ecofriendly and efficient energy management [34]. The thermoelectric properties of RhCrX (X = Si, Ge, P, As) compounds are calculated by the BoltzTrap code [35], which is related to the semiclassical Boltzmann theory and rigid band approach. In this study, we calculated the electrical conductivity σ, thermal conductivity κ, Seebeck coefficient *S*, thermopower factor *PF* and figure of merit *ZT* and the results are plotted in Fig. 7 and Fig. 8. An efficient thermoelectric material is required to have high electrical conductivity, a low thermal conductivity and a large Seebeck coefficient. To our information, the thermoelectric efficiency for the considered compounds has not been surveyed till now. The combined results of both spin channels to estimate overall thermal conductivity *κ*, electrical conductivity *σ*, Seebeck coefficient *S*, power factor *PF* and figure of merit *ZT*, can be expressed [36] respectively by:

$$\sigma = \sigma(\uparrow) + \sigma(\downarrow) \tag{15}$$

$$\kappa = \kappa(\uparrow) + \kappa(\downarrow) \tag{16}$$

$$\mathrm{S} = [S(\uparrow).\sigma(\uparrow) + S((\downarrow).\sigma(\downarrow)]/[\sigma(\uparrow) + \sigma(\downarrow)] \tag{17}$$

$$PF = S^2\sigma = S(\uparrow)^2.\sigma(\uparrow) + \mathrm{S}((\downarrow)^2.\sigma(\downarrow) \tag{18}$$

$$ZT = \mathrm{T}.S^2.\sigma/\kappa \tag{19}$$

The variation of the electrical conductivity σ as a function of temperature is plotted in Fig. 7(a). We see that the electrical conductivity increases mostly linearly with temperature for all compounds. This could be justified by the fact that increasing temperature enhances thermal energy of the electrons to freely form a high-conducting state.

Fig. 7(b) displays the temperature dependence of thermal conductivity *κ*. The *κ* plots follow a similar trend as those of electrical conductivity σ. The *κ* value increases gradually from nearly zero for all four materials in the range of temperature between 100K and 600K. Beyond these temperatures, there is almost a linear increase in the range studied. The rise of thermal conductivity with increasing temperature is mainly due to the higher charge carrier concentration. Note in passing that the nearly indistinguishable plots (Fig. 7(a,b)) suggest that RhCrP and RhCrAs should have approximately the same band gaps (1.01 and 1.06 eV, respectively). We also computed the total Seebeck coefficient *S* variation calculated by two-current model [36] to designate its nature as shown in Fig. 8 (a,b). As one can see, the Seebeck coefficient of both RhCrSi and RhCrGe Heusler compounds is negative for the entire temperature range and negative in both RhCrP and RhCrAs Heusler compounds. The negative sign of *S* explains that electrons are the dominant charge carriers and the positive sign of *S* explains that the holes are dominant charge carriers. Therefore, the RhCrSi and RhCrGe compounds are *n*-type materials and the RhCrP and RhCrAs compounds are *p*-type materials. The power factor (*PF*) was evaluated in order to determine the performance of RhCrX (X = Si, Ge, P, As) compounds as thermoelectric materials, where a large PF denotes that large voltages and currents are generated. The *PF* is shown as a function of temperature in Fig. 8(c), which clearly demonstrates that PF increases gradually with temperature, suggesting its potential stand for commercial thermoelectric applications. Finally, the calculated transport coefficients are now used to estimate the thermoelectric efficiency through the figure of merit *ZT* measurement. The materials are considered as good elements for thermoelectric devices if their *ZT* is about or greater than unity [37].

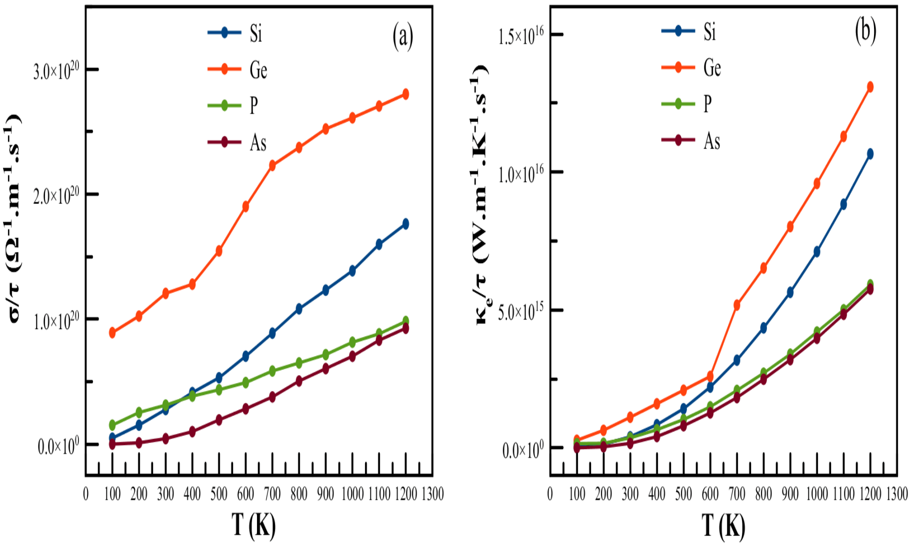

FIG. 7. Calculated transport coefficients of RhCrZ (Z= Si, Ge, P, As) (a) electrical conductivity σ/τ and (b) electronic thermal conductivity κ_e/τ (where τ is the relaxation time) as a function of temperature.

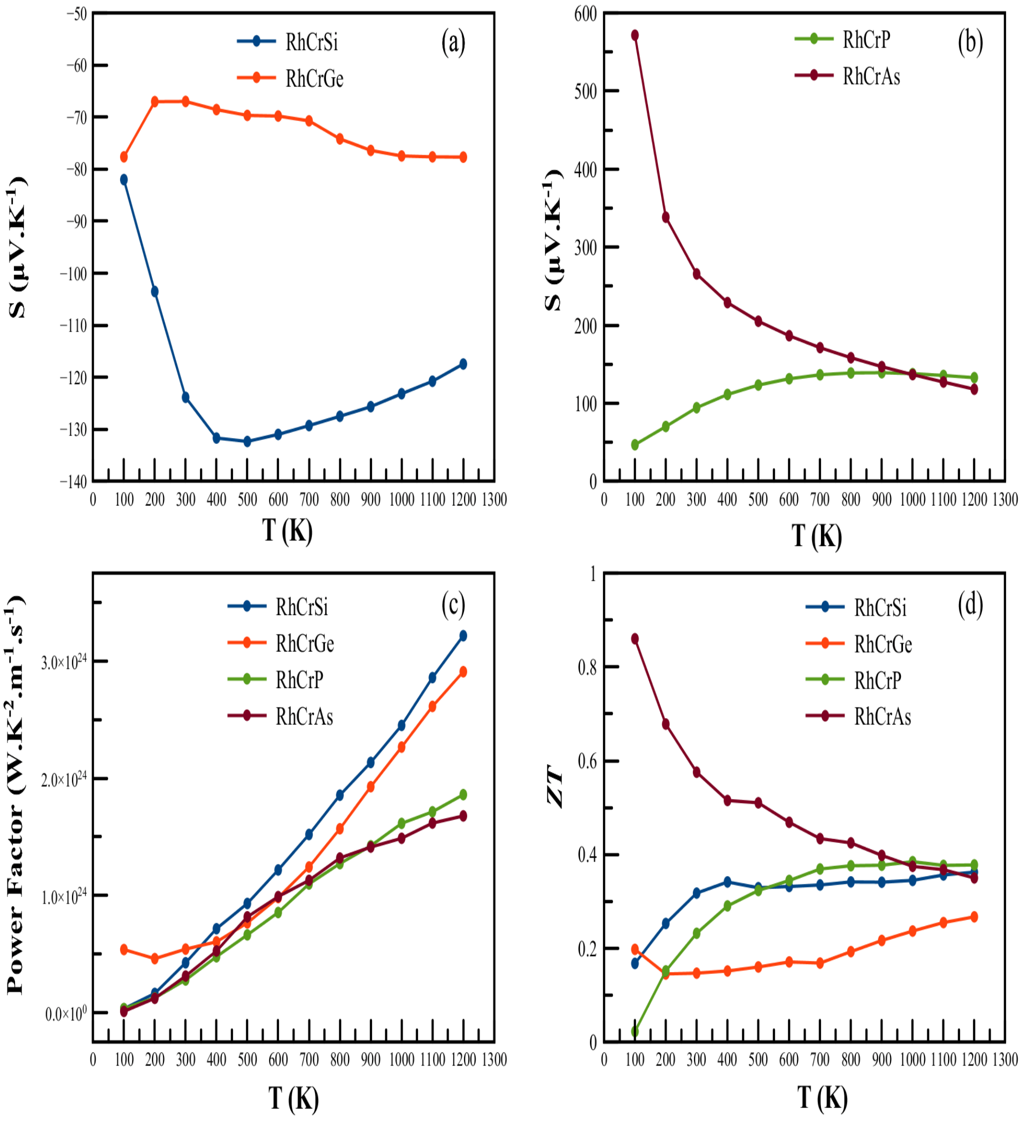

FIG. 8. Calculated transport coefficients of RhCrZ (Z= Si, Ge, P, As) (a,b) Seebeck coefficient (S), (c) power factor (*PF*) and (d) figure of merit (*ZT*), as a function of temperature.

The variation of *ZT* is shown in Fig. 8(d), which shows a linearly increasing trend with temperature in the three RhCrSi, RhCrGe and RhCrP compounds and a decrease in the RhCrAs compound. The highest value of 0.86 is reached for RhCrAs at 100K, where the Seebeck coefficient reaches its maximum (Fig. 8(a)). This value is the same compared to that of thermoelectric materials, such as Sb_2Te_3 (*ZT*~0.9) found at ~273K [38] and zintl compounds Ba_3AlAs_3 (*ZT* = 0.74) and Sr_3AlAs_3 (*ZT* = 0.85) found at 100K and 150K, respectively [39]. In return, the value for RhCrP at 100K is smaller due to the lower Seebeck coefficient at the same temperature. At room temperature, the computed thermoelectric efficiency of RhCrAs (*ZT* = 0.568) is nearly greater than the range of the few half-Heusler alloys studied experimentally as 0.45 [40, 41] and may trigger its stand as potential candidate for a thermoelectric material.

Although the observed *ZT* values are small for the three RhCrSi, RhCrGe and RhCrP compounds compared to available thermoelectric materials, the thermoelectric performance of the present materials could be improved by doping with suitable *sp*-elements or miniaturizing the size; i.e., shifting to nano-dimensions [42,43]. Therefore, the present materials are likely to find their application as high temperature thermoelectric materials. The values of electrical conductivity, thermal conductivity and Seebeck coefficient at room temperature are summarized in Table 5. Based on these types of results, RhCrAs can be considered to be probably the most noticeable material for thermoelectric applications. Unfortunately, a comparison of our results is not achieved due to lack of any experimental data regarding these materials. Exactness and contrast are not possible, but these calculations may act as reference data and expand the valuable information to forthcoming theoretical or experimental investigations.

Table 5. Values of electrical conductivity σ (in 10^{19} $\Omega^{-1}.m^{-1}.s^{-1}$), thermal conductivity κ (in 10^{14} $W.m^{-1}.K^{-1}.s^{-1}$), Seebeck coefficient *S* (in $\mu V.K^{-1}$), power factor (*PF*) (in 10^{23} $W.m^{-1}.K^{-2}.s^{-1}$) and figure of merit *ZT* at 300 K for RhCrZ (Z= Si, Ge, P, As) compounds.

Compound	σ	κ	*S*	*PF*	*ZT*
RhCrSi	2,770	4,016	-123,850	4,249	0,317
RhCrGe	12,060	11,082	-67,001	5,414	0,146
RhCrP	3,120	3,603	94,418	2,782	0,232
RhCrAs	0,441	1,623	265,738	3,115	0,575

Conclusion

In conclusion, the electronic structure, magnetic and thermoelectric properties of the half-Heusler alloys RhCrZ (Z= Si, Ge, P, As) have been calculated using the first-principles full-potential linearized augmented plane waves (FPLAPW+lo) method within the generalized gradient approximation (GGA). In all compounds, the stable type α + FM configuration structure was energetically more favorable than type β and type γ structures. Elastic properties show that all our compounds have good mechanical strength and good thermal stability with ductile nature, especially if they are used in a thermoelectric generator. At the equilibrium lattice constant, our GGA calculations have shown that RhCrZ (Z= Si, Ge, P, As) are half-metallic ferromagnets (HMFs) with a half-metallic gap E_{HM} of 0.37, 0.35, 0.25 and 0.02 eV for RhCrSi, RhCrGe, RhCrP and RhCrAs, respectively. The total spin magnetic moment per formula unit in μ_B follows the rule $\mu_{tot} = Z_t - 18$. The half-metallicity is found to be robust with respect to the lattice compression and is maintained up to the lattice-constant contraction of -3.37%, -3.77%, -5.56% and -8.77% for RhCrSi, RhCrGe, RhCrP and RhCrAs, respectively. Further, the transport properties of the materials reveal some fruitful results. These materials exhibit high values of Seebeck coefficient and power factor with room temperature values. The computed figure of merit showed an extensive variety of temperatures demonstrating that HH RhCrAs exhibits a preferred thermoelectric conduct over other HH RhCrSi, RhCrGe and RhCrP materials. Since these materials offer high spin-polarization, robust half-metallicity and high Seebeck coefficient, this makes them credible applicants for spintronic and thermoelectric applications. To the best of our knowledge, most of the investigated properties are reported for the first time and provide a reference for future experimental work.

Acknowledgments

This work has been supported by the PRFU project (N° B00L02UN220120190013) of the Ministry of Higher Education and Scientific Research (MESRS) and the Directory General of Scientific Research and Technological Development (DGRST).

References

[1] Casper, F., Graf, T., Chadov, S., Balke, B. and Felser, C., Semicond. Sci. Technol., 27 (2012) 06300.

[2] Akasaka, M., Iida, T., Matsumoto, A., Yamanaka, K., Takanashi, Y., Imai, T. and Hamada, N., J. Appl. Phys., 104 (2008) 013703.

[3] Downie, R.A., Barczak, S.A., Smith, R.I. and Bos, J.W.G., J. Mater. Chem. A., 2 (2014) 6107.

[4] deGroot, R.A., Mueller, F.M., van Engen, P.G. and Buschow, K.H.J., Phys. Rev. Lett., 20 (1983) 2024.

[5] Lv, S., Li, H., Han, D., Wu, F., Liu, X. and Meng, J., J. Magn. Magn. Mater., 323 (2011) 416.

[6] Saeed, Y., Nazir, S., Shaukat, A. and Reshak, A.H., J. Magn. Magn. Mater., 322 (2011) 3214.

[7] Galanakis, I. and Mavropoulos, P., Phys. Rev. B, 67 (2003) 104417.

[8] Kandpal, H.C., Fecher, G.H. and Felser, C.J., J. Phys. D: Appl. Phys., 40 (2007) 1507.

[9] Chen, J., Gao, G.Y., Yao, K.L. and Song, M.H., J. of Alloys and Compounds, 509 (2011) 10172.

[10] Zhang, L., Cheng, Z. X., Wang, X. T., Khenata, R. and H. Rozale, J. Supercond. Nov. Magn., 31 (2018) 189.

[11] Galanakis, I., Dederichs, P. H. and Papanikolaou, N., Phys. Rev. B, 66 (2002) 134428.

[12] Youn, S. J. and Min, B. I., Phys. Rev. B, 51 (1995) 10436.

[13] Kervan, S. and Kervan, N., Intermetallics, 19 (2011) 1642.

[14] Fang, T., Zheng, S., Zhou, T., Yana, L. and Zhang, P., Phys. Chem. Chem. Phys., 19 (2017) 4411.

[15] Bhat, T.M. and Gupta, D.C., Journal of Physics and Chemistry of Solids, 119 (2018) 281.

[16] Wei, J. and Wang, G., Journal of Alloys and Compounds, 757 (2018) 118e123.

[17] Qiu, P., Yang, J., Huang, X., Chen, X. and Chen, L., Appl. Phys. Lett., 96 (2010) 152105.

[18] Hohenberg, P. and Kohn, W., Phys. Rev. B, 136 (1964) 864.

[19] Wimmer, E., Krakauer, H., Weinert, M. and Freeman, A.J., Phys. Rev. B, 24 (1981) 864.

[20] Blaha, P., Schwarz, K., Madsen, G.K.H., Kvasnicka, D. and Luitz, J., WIEN2k, An Augmented Plane Wave+Local Orbitals Program for Calculating Crystal Properties (Technische Universität Wien, 2001).

[21] Perdew, J.P., Burke, S. and Ernzerhof, M., Phys. Rev. Lett., 77 (1996) 3865.

[22] Graf, T., Felser, C. and Parkin, S.S.P., Progress Solid State Chem., 39 (2011) 1.

[23] Murnaghan, F.D., Proc. Natl. Acad. Sci. USA, 30 (1944) 244.

[24] Ma, J., Hegde, V.I., Munira, K., Xie, Y., Keshavarz, S., Mildebrath, D.T., Wolverton, C., Ghosh, A.W. and Butler, W. H., Phys. Rev. B, 95 (2017) 024411.

[25] Ahmad, R. and Mehmood, N., J. Supercond. Nov. Magn., 31 (2017) 2637.

[26] Mehmood, N., Ahmad, R. and Murtaza, G., J. Supercond. Nov. Magn., 30 (2017) 2481.

[27] Sinko, G.V. and Smirnov, N.A., J. Phys. Condens. Matter, 14 (2002) 6989.

[28] Hill, R., Proc. Phys. Soc. Lond., 65 (1953) 909.

[29] Pugh, S.F., Philos. Mag., 45 (1954) 823.

[30] Fine, M.E., Brown, M.D. and Marcus, H.L., Scr. Metall, 18 (1984) 951.

[31] Galanakis, I., Mavropoulos, P. and Dederichs, P.H., J. Phys. D. Appl. Phys., 39 (2006) 765.

[32] Sato, K., Dederichs, P.H., Yoshida, H.K. and Kudrnovsky, J., J. Phys.: Condens. Matter, 16 (2004) S5491.

[33] Şasioğlu, E., Sandratskii, L.M. and Bruno, P., J. Phys.: Condens. Matter, 17 (2005) 995.

[34] Khandy, S.A. and Gupta, D.C., J. Magn. Magn. Mater., 441 (2017) 166.

[35] Madsen, G.K.H. and Singh, D.J., Phys. Commun., 175 (2006) 67.

[36] Xiang, H.J. and Singh, D.J., Phys. Rev. B, 76 (2007) 195111.

[37] Takeuchi, T., Mater. Trans., 50 (2009) 2359.

[38] G. J. Snyder and E.S. Toberer, Nature Materials, 7, 105, (2008).

[39] Bekhti-Siad, A., Bettine, K., Rai, D. P., Al-Dourid, Y., Wang, X., Khenata, R., Bouhemadou, A. and Voon, C.H., Chinese J. Physics, 56 (2018) 870.

[40] Hsu, C.C., Liu, Y.N. and Ma, H.K., J. of Alloys and Compounds, 597 (2014) 217.

[41] Wang, D., Wang, G. and Li, W., J. of Alloys and Compounds, 692 (2017) 599.

[42] Khandy, S.A. and Gupta, D.C., J. Magn. Magn. Mater., 441 (2017), 166.

[43] Geng, H. and Zhang, H., J. Appl. Phys., 116 (2014) 033708.